Second-Generation Meridianin Analogues Inhibit the Formation of *Mycobacterium smegmatis* Biofilms and Sensitize Polymyxin-Resistant Gram-Negative Bacteria to Colistin

Michael J. Zeiler,[a] Roberta J. Melander,[a] and Christian Melander*[a]

Drug-resistant bacteria are rapidly becoming a significant problem across the globe. One element that factors into this crisis is the role played by bacterial biofilms in the recalcitrance of some infections to the effects of conventional antibiotics. Bacteria within a biofilm are highly tolerant of both antibiotic treatment and host immune responses. Biofilms are implicated in many chronic infections, including tuberculosis, in which they can act as bacterial reservoirs, requiring an arduous antibiotic regimen to eradicate the infection. A separate, compounding problem is that antibiotics once seen as last-resort drugs, such as the polymyxin colistin, are now seeing more frequent usage as resistance to front-line drugs in Gram-negative bacteria becomes more prevalent. The increased use of such antibiotics inevitably leads to an increased frequency of resistance. Drugs that inhibit biofilms and/or act as adjuvants to overcome resistance to existing antibiotics will potentially be an important component of future approaches to antibacterial treatment. We have previously demonstrated that analogues of the meridianin natural product family possess adjuvant and antibiofilm activities. In this study, we explore structural variation of the lead molecule from previous studies, and identify compounds showing both improved biofilm inhibition potency and synergy with colistin.

Introduction

Antibiotic resistance has become one of the largest threats to the medical community.[1] In 2019, the Centers for Disease Control and Prevention (CDC) reported 2.8 million cases of drug-resistant infections, 35000 of which resulted in death.[2] As resistance to an antibiotic increases past its breakpoint, defined by the Clinical and Laboratory Standards Institute (CLSI) as the minimum inhibitory concentration (MIC) of the antibiotic corresponding to therapeutically achievable levels, effective in vivo concentrations can no longer be achieved, and the infection becomes untreatable with that antibiotic. As a consequence of its well-documented side effects, colistin is typically prescribed as a last-resort drug to treat infections caused by multidrug-resistant (MDR) Gram-negative bacteria.[3] However, resistance to colistin has been observed worldwide, highlighting the need for alternative approaches to combat MDR Gram-negative infections. With the output of new antibiotics unable to keep up with the rapid development of resistance, orthogonal strategies are being explored to combat this problem.

One of these approaches involves the use of antibiotic adjuvants. This approach involves circumventing bacterial defense mechanisms in order to re-sensitize bacteria to approved antibiotics. Adjuvants are non-microbicidal compounds that target non-essential bacterial functions in order to potentiate the activity of antibiotics. By targeting non-essential pathways, adjuvants potentially exert reduced selective pressure on bacteria, thus slowing the development of resistance. Overall, adjuvants hold the potential to enable the use of old antibiotics previously rendered obsolete by resistance and provide an avenue to help resolve the current problem of a limited antibiotic pipeline.

Another important mechanism that is frequently associated with increased drug tolerance is the formation of biofilms. Bacterial biofilms are defined as a surface attached community of bacteria encased in an extracellular matrix of biomolecules (polysaccharides, proteins, DNA, and lipids). Bacteria in a biofilm can exhibit a 1000-fold increase in drug tolerance compared to those in a free-floating (planktonic) state.[4]. Multiple factors contribute to this tolerance. The matrix itself acts as a physical barrier between the bacteria and the outside environment, including some antibacterial drugs and the host immune response. Furthermore, many cells within the biofilm have reduced metabolic activity, which decreases the efficacy of antibiotics that target cell reproduction and growth.[4] In addition, the increased cellular density within biofilms increases the frequency of horizontal gene transfer (HGT). Increased HGT rates lead to increased acquisition and spread of antibiotic resistance.

It has been postulated that latent reservoirs of *Mycobacterium tuberculosis*, the causative agent of tuberculosis (TB), exist in a biofilm-like state within infected individuals. For example, it has been demonstrated that *M. tuberculosis* can form biofilm-like communities on cellular debris (which mimics the environment of lung lesions in TB patients) and subsequently exhibit

[a] M. J. Zeiler, Prof. R. J. Melander, Prof. C. Melander
Department of Chemistry and Biochemistry
University of Notre Dame, Notre Dame, IN 46556 (USA)
E-mail: cmelande@nd.edu

Supporting information for this article is available on the WWW under https://doi.org/10.1002/cmdc.202000438

isoniazid tolerance.[5] The World Health Organization (WHO) attributed 1.5 million deaths to TB in 2019 alone.[6] Treatment of drug-susceptible TB is a long process that lasts a minimum of six months where patients undergo antibiotic combination therapy with isoniazid, rifampicin, and pyrazinamide.[7] Challenges with this regimen include substantial drug toxicity and ensuring patient compliance. The lengthy regimen is due in part to the necessity of eradicating latent reservoirs to avoid disease rebound.[5] MDR TB infections are caused by strains that have acquired genetic resistance to both of the front-line drugs: isoniazid and rifampicin, in addition to drug tolerance due to the formation of biofilms. With the frequency of MDR-TB cases increasing, the CDC has marked MDR-TB as a serious problem in the coming decades.[2] Though challenging, targeting bacteria in a biofilm state is one approach for combatting TB and could potentially shorten the treatment regimen, which would increase patient compliance, and in turn slow resistance acquisition.

Due to the pathogenicity of *M. tuberculosis*, *Mycobacterium smegmatis* is often used as a model bacterium because it is non-pathogenic and faster growing. In addition, *M. smegmatis* shares over 2000 genetic homologues with *M. tuberculosis*, such as cell-wall composition and many cellular functions.[7] We have previously demonstrated that activity against *M. smegmatis* often translates to activity against *M. tuberculosis*.[8,9]

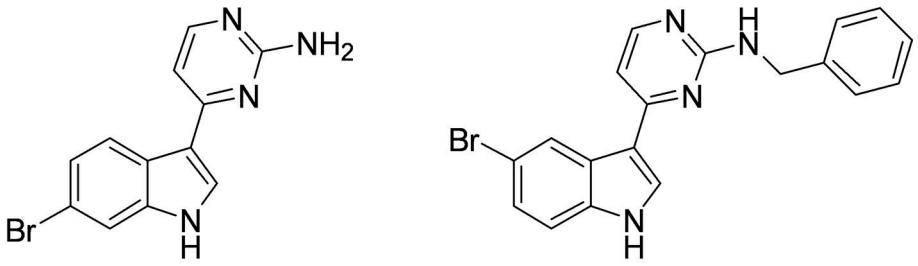

1 **2**

Figure 1. Meridianin D and lead analogue 2.

Recently, we reported that analogues of the marine natural product meridianin D, **1** (Figure 1), inhibit and disperse biofilms of *M. smegmatis*.[10] Lead compound **2** was shown to be superior to 1 and demonstrated the ability to inhibit biofilms at low micromolar concentrations as well as the ability to disperse preformed biofilms. Separately, lead compound 2 displayed the ability to re-sensitize Gram-negative bacteria to colistin.[11] Probing this activity, we wanted to create a pilot library that diversified the structure of our lead compound 2 in order to potentially improve its potency both against mycobacterial biofilms and as an adjuvant for colistin against Gram-negative bacteria. Our studies focused on the pendent phenyl ring, by adding electron-withdrawing (EWG) and electron-donating (EDG) groups with various substitution patterns to probe the steric and electronic effects of this ring on activity. We also determined activity based on the position of the bromide, and the relative orientation of the 2-aminopyrimidine (2-AP).

Results and Discussion

The pilot library based on lead analogue **2** was synthesized according to previously reported methods (Scheme 1).[11] 5-Bromo indole was acylated with acetyl chloride to afford the corresponding C3-acylated indole, which was then protected with *p*-toluene sulfonyl chloride (TsCl) to give the tosyl-protected indole. 6-Bromo indole underwent the same reaction sequence to afford the corresponding tosyl-protected indole. The tosyl-protected indoles were reacted with *N,N*-dimethylformamide dimethyl acetal (DMF-DMA) to generate their corresponding vinylogous amide products (**3a** and **3b**), which were cyclized with the appropriate benzylguanidine derivatives to produce the 2-aminopyrimidine final products **4a**–**n**. Variation of the benzylguanidines was achieved by reacting *S*-methyl isothiourea hemisulfate with commercially available benzylamines to form benzylguanidine sulfates that were then used in the formation of the 2-aminopyrimidine rings.[12]

Further derivatization of lead analogue **2** was achieved with attachment of the 2-AP at C5 rather than C4 (Scheme 2). To access these derivatives, 5-bromo indole was halogenated at C3

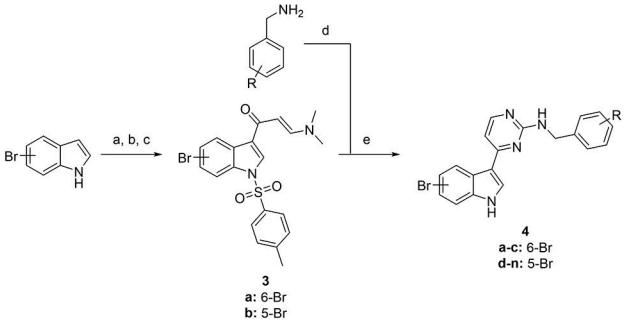

Scheme 1. Synthesis of C4-substituted derivatives: a) acetyl chloride, $SnCl_4$, toluene; b) TsCl, DIPEA, DMAP, CH_2Cl_2; c) DMF-DMA, toluene; d) *S*-methyl isothiourea, H_2O, EtOH; e) benzylguanidine, K_2CO_3, 2-methoxyethanol; f) HCl, MeOH

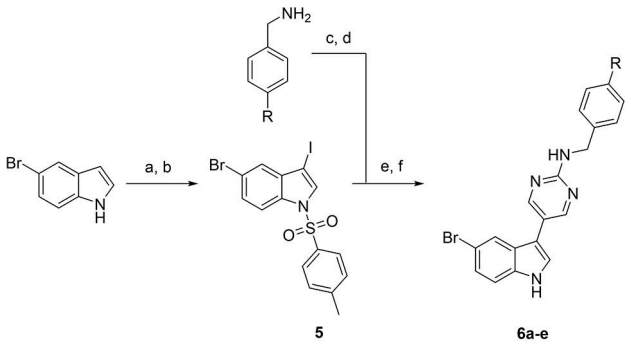

Scheme 2. Synthesis of C5-substituted analogues. a) NIS, TEA, CH_2Cl_2; b) TsCl, DIPEA, DMAP, CH_2Cl_2; c) 2-fluoro-5-bromo pyrimidine, TEA, DMF; d) B_2Pin_2, KOAc, Pd(dppf)Cl_2, dioxane; e) Pd(PPh_3)$_4$, K_2CO_3, toluene, EtOH; f) Cs_2CO_3, THF, MeOH.

using *N*-iodosuccinimide to form the corresponding C3-iodo indole, which was then protected with TsCl as described previously to afford compound **5**.[13] The 2-benzylamino-5-pyrimidinyl boronic acid pinacol esters (Bpin) were synthesized by treating the desired, commercially available benzylamines with 2-fluoro 5-bromo pyrimidine followed by a Miyaura borylation to install a Bpin group[14] In the case of the methyl ester derivative, **6c**, the ester used was synthesized by a Fischer esterification of 4-aminomethyl benzoic acid to afford the methyl ester as its corresponding hydrochloride salt. The pyrimidines were then coupled to the tosyl-protected indole (**5**) using Suzuki-Miyaura cross-coupling conditions.[13] Deprotection of the tosylates was achieved by treatment with cesium carbonate to yield desired final products **6a**–**e**.[15]

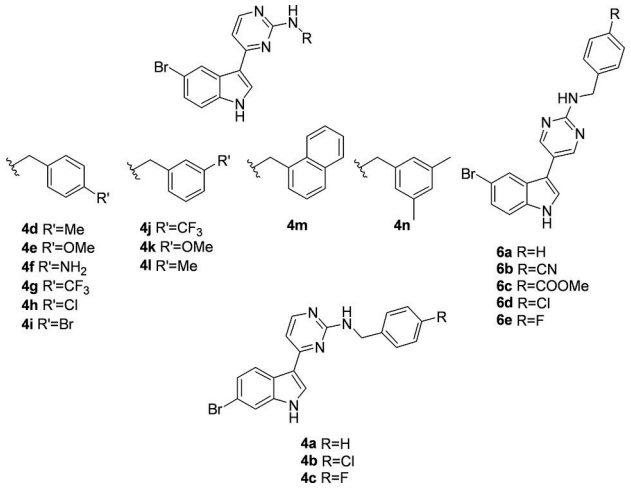

Figure 2. Pilot library of lead analogue **2**.

Table 1. Biofilm inhibition values in *M. smegmatis*.

Compound	IC_{50} [μM]	Compound	IC_{50} [μM]
2	6.9 ± 0.8	**4j**	> 20
4a	16.6 ± 1.8	**4k**	> 20
4b	17.1 ± 5.8	**4l**	10.4 ± 4.4
4c	8.5 ± 1.4	**4m**	> 20
4d	19.1 ± 1.9	**6a**	7.9 ± 2.3
4e	5.9 ± 1.3	**6b**	> 20
4f	14 ± 5	**6c**	> 20
4g	18 ± 3.5	**6d**	> 20
4h	4.5 ± 1.7	**6e**	> 20
4i	5.6 ± 2.1		

With the pilot library in hand (Figure 2), we began testing all 20 compounds for anti-biofilm activity in *M. smegmatis*. The library was tested for microbicidal activity and proved to be nontoxic, with most compounds possessing MIC's ≥ 200 μM. All compounds were tested in a crystal violet reporter assay to determine their IC_{50} values (Table 1). The parent compound, **2**, returned an IC_{50} of 6.9 μM. Compound **4h** was discovered to be the most active biofilm inhibitor, with an IC_{50} value of 4.5 μM, followed by an IC_{50} of 5.6 μM for compound **4i**. In general, compounds containing an EWG on the C4 position of the phenyl ring (**4b**, **4c**, **4h**, **4j**) proved to be more active than those with an EDG (Table 1). For example, compounds **4d**, and **4f**, which incorporated EDGs, exhibited higher IC_{50} values than the parent compound **2**. In addition, increasing the steric bulk of the substituent (i.e., installation of naphthyl (**4o**)) diminished activity substantially, displaying an IC_{50} value of > 20 μM (Table 1).

Changing the attachment position between the indole and the pyrimidine to the C5 position on the 2-AP (compound **6a**) from the C4 position (compound **2**) conferred no significant change in activity. However, the incorporation of substituents on the benzyl groups (compounds **6b**–**6e**) diminished biofilm inhibition activity compared to the unsubstituted compound **6a** (Table 1).

It was previously reported that meridianin D **1** and parent compound **2** demonstrated adjuvant activity with colistin in Gram-negative bacteria.[11] Therefore, all 20 compounds from this library were tested with colistin against polymyxin-resistant strains of *Klebsiella pneumoniae* (KP) and *Acinetobacter baumannii* (AB). Compounds were first tested individually to ensure they had no microbicidal effects on planktonic cells, by recording their MIC values. All compounds proved to be non-microbicidal alone with MIC values greater than 200 μM (Table S2 in the Supporting Information). The library was then assayed at subinhibitory concentrations for their ability to potentiate colistin against the resistant KP and AB strains.

Several compounds showed adjuvant activity at 60 μM, with several possessing potency either greater than or comparable to the parent compound **2** (Table 2). Analogues **4l** and **4g** demonstrated the greatest activity, lowering the colistin MIC from 1024 to 2 and 4 μg/mL, respectively, in *A. baumannii* 4106 and from 512 to 0.5 μg/mL for both in *K. pneumoniae* B9 (Table 2). Inspired by the significant activity of the C3-methyl-

Table 2. Colistin MIC values [μg/mL] with **4n**, **4h** and **4p** at 60 μM.

Compound	*A .baumannii* 4106	*K. pneumoniae* B9
–	1024	512
2	2	0.5
4l	2	2
4g	4	0.5
4n	> 32	> 16

Table 3. Dose-response of **2** and **4g** for colistin MIC values [μg/mL].

[Cpd] μM	*A. baumannii* 4106		*K. pneumoniae* B9	
	2	**4g**	**2**	**4g**
60	2	4	0.5	0.5
30	2	4	0.5	0.5
15	2	4	1	0.5
10	8	4	4	0.5
7.5	32	4	8	1
5	>32	8	>16	2

substituted analogue (**4l**), we wanted to see if creating symmetry on the phenyl ring would affect adjuvant activity by synthesizing the 3,5-dimethyl-substituted analogue **4n**. Compound **4n**, however, showed negligible activity, with a colistin MIC of ≥16 μg/mL at 60 μM for both AB and KP strains.

The parent compound 2 was unable to bring the colistin MIC below the breakpoint when dosed at lower concentrations. The addition of a CF_3 group, however, to the *para* position of the phenyl ring (**4g**) improved the dose-response activity of the molecule (Table 3). While having comparable activity to 2 at 60 μM, **4g** was able to maintain the colistin MIC at 4 μg/mL down to 7.5 μM in *A. baumannii* 4106. Dose-response was improved further in *K. pneumoniae* B9, holding colistin below or at its breakpoint (2 μg/mL) down to 5 μM, effectively making the colistin-resistant strain susceptible and once again potentially treatable with colistin. It is worth noting that shifting the CF_3 substitution from a *para* orientation (**4g**) to a *meta* orientation (**4j**) made the molecule significantly less active, with a colistin MIC of >32 μg/mL in *A. baumannii* 4106 and >16 μg/ml in *K. pneumoniae* B9 (Table S3).

Conclusion

In conclusion, structure-activity relationship (SAR) studies were performed on a previously reported meridianin analogue **2**, generating several analogues with enhanced activities. Members of the synthesized library showed improved ability to inhibit biofilm formation in *M. smegmatis*, relevant for the potential application for the treatment of TB. In general, installation of halogens at the *para* position of the phenyl ring led to increased activity, where halogens displayed the greatest biofilm inhibiting activity. Electron-donating groups, with the exception of *para*-methoxy, had deleterious effects on biofilm inhibition activity. In addition, several compounds were able to potentiate colistin against two clinically relevant, colistin-resistant Gram-negative bacterial strains, *A. baumannii* 4106 and *K. pneumoniae* B9. It was shown that taking an active *meta*-methylated phenyl head group and introducing symmetry through a 3,5-dimethyl substitution pattern effectively abolished colistin potentiation activity. However, **4g**, which introduced a CF_3 group onto the *para* position of the phenyl ring, lowered the colistin MIC to its breakpoint at an adjuvant concentration of 5 μM, thus exceeding the activity of the previous lead analogue **2**. Further SAR studies are planned to implement these preliminary findings in creating more potent analogues for both mycobacterial biofilm inhibition, including against *M. tuberculosis*, and as adjuvants for colistin. Additionally, future work will be conducted to improve water solubility, as this area could hinder future development.

Experimental Section

Chemistry experimental: All reagents were purchased from commercially available sources without further purification. Flash chromatography was performed using 60 Å mesh standard grade silica gel from Sorbetch. NMR solvents were obtained from Cambridge Isotope Labs and used as is. All ^{1}H NMR (400 MHz) were recorded at 25 °C on a Bruker Avance spectrometer. All ^{13}C NMR (101 and 201 MHz) spectra were also recorded at 25 °C on Bruker Avance spectrometers. Chemical shifts (δ) are given in parts per million (ppm) relative to the respective NMR solvent. All high-resolution mass spectrometry measurements were made in the Mass Spectrometry and Proteomics Facility at the University of Notre Dame. Infrared spectra were obtained on a FT/IR-4100 spectrophotometer (ν_{max} in cm^{-1}). UV absorbance was recorded on a Genesys 10 scanning UV/visible spectrophotometer (λ_{max} in nm).

General Synthetic Procedures

Benzyl guanidine formation: The appropriately substituted benzylamine (1 g, 1 equiv) was added to a stirring solution of *S*-methyl isothiourea hemi-sulfate (1 equiv) in H_2O/EtOH (1:1, 2 M to benzylamine), and the reaction mixture was heated at 80 °C under a condenser overnight. The mixture was cooled to room temperature. Diethyl ether was added to the mixture until a white solid was observed, then the mixture was placed in a refrigerator at 5 °C for 1 h. The resulting white solid was filtered and washed further with diethyl ether to afford the substituted benzylguanidine sulfates as a white solid (80%). Used without further purification.

General procedure for acylation of indole: Indole (5 g, 1 equiv) was dissolved in toluene (0.2 M) then acetyl chloride (2 equiv) was added. Tin(IV) chloride (2 equiv) was added slowly at 0 °C. The reaction mixture was warmed slowly to room temperature and stirred for 2 h. TLC in hexanes/EtOAc (1:1) showed absence of starting material. The reaction was quenched with saturated sodium bicarbonate to neutral pH then extracted with EtOAc. The organic layer was washed with water then brine (2x) and dried over magnesium sulfate. Solvent was removed under reduced pressure. The residue was purified over silica gel with hexanes/EtOAc (4:1). The resulting solid was washed with cold MeOH to afford the product. NMR taken in $CDCl_3$.

N-Tosyl protection of indole: 3-Acetyl Indole (4.8 g, 1 equiv), *p*-toluenesulfonyl chloride (1.5 equiv), DIPEA (2 equiv), and DMAP (0.05 equiv) were stirred in CH_2Cl_2 (0.2 M to indole) at room temperature overnight. The reaction mixture was washed with water and brine (2x) and dried over magnesium sulfate, then solvent was removed under reduced pressure. The residue was purified over silica gel with hexanes/EtOAc (7:1) to afford a white solid.

Vinylogous amide formation: *N*-Tosyl 3-acetyl indole (6.6 g, 1 equiv) was dissolved in toluene (0.4 M to indole) followed by addition of DMF-DMA (1,1-dimethoxy-*N*,*N*-dimethylmethanamine) (2 equiv) and heated at 90 °C overnight. After cooling the reaction to room temperature reaction was diluted with EtOAc then washed with water and brine (2x) and dried over magnesium sulfate. Solvent was removed under reduced pressure and the residue was

purified over silica gel with hexanes/EtOAc (1:1) to afford the product as a bright yellow solid. NMR taken in $CDCl_3$.

2-Amino pyrimidine formation: Vinylogous amide (600 mg, 1 equiv), the appropriate benzyl-guanidine sulfate (2 equiv) and potassium carbonate (2.1 equiv) were dissolved in 2-methoxy ethanol (22 mM to vinylogous amide) and stirred at 130 °C overnight. After cooling to room temperature, reaction was diluted with EtOAc and washed with water and brine (2×), dried over magnesium sulfate, and solvent was removed under reduced pressure. The resulting residue was purified over silica gel with hexanes/EtOAc (1:1). The resulting off-white solid was washed multiple times with both diethyl ether and warm hexanes.

C-3 Iodination of indole: To a stirring solution of 5-Br Indole (1.5 g, 1 equiv) in CH_2Cl_2 (0.2 M to indole) was added TEA (1 equiv). After 30 min, *N*-iodosuccinimide (1 equiv) was added. The reaction mixture was stirred at room temperature overnight then quenched with saturated sodium thiosulfate, washed with water and brine (2x), dried over magnesium sulfate and solvent was removed under reduced pressure. The resulting residue was purified over silica gel with hexanes/EtOAc (7:1) to afford the product as a light lavender-colored solid.

Fischer esterification of 4-(aminomethyl) benzoic acid: To a stirring mixture of 4-(aminomethyl) benzoic acid (1 g, 1 equiv.) in MeOH (0.2 M to benzoic acid) was added slowly conc. HCl (1 equiv). The resulting solution was then refluxed at 85 °C for 16 h. The reaction was cooled to room temperature and the MeOH was removed under vacuum repeatedly to remove any excess HCl. Product afforded as a white solid (95%) and used without any further purification.

Nucleophilic aromatic substitution of 2-fluoro-5-bromopyrimidine: To a stirred solution of 2-fluoro 5-bromo pyrimidine (1 g, 1 equiv), and DIPEA (4 equiv) in DMF (0.3 M to pyrimidine) was added slowly the appropriate benzylamine (2 equiv), and the reaction mixture was heated to 85 °C for 1 h. After the mixture had cooled to room temperature, water was added until precipitate was observed. The flask was placed in a refrigerator at 5 °C for 1 h. The solid was filtered and washed with excess water to remove remaining DMF then dried under vacuum. Crude product used without further characterization.

Miyaura borylation: To a flame-dried RBF was added the appropriate 2-amino pyrimidine (1 g, 1 equiv), B_2Pin_2 (1.1 equiv) and KOAc (3 equiv). The flask was evacuated under vacuum and backfilled with argon. This was repeated 3x. Anhydrous dioxane (0.2 M to pyrimidine) was added and stirred for 5 min. Argon was then bubbled through for 15 min before the addition of Pd(dppf)Cl_2 (0.05 equiv). Following addition of catalyst, argon was further bubbled through for another 5 min. The mixture was refluxed under argon at 115 °C for 4 h which after completion had taken on a black color. EtOAc was added, sonicated, and filtered. The organic layer was washed with water and brine and run through a plug of silica with EtOAc. After removal of solvent the remaining solid was columned over silica in hexanes with 0–50% EtOAc to remove any remaining baseline impurities, affording a solid which was washed with EtOH three times to afford the product as a fine, white solid (50%). Used without further purification.

Suzuki cross-coupling of indole and pyrimidine: 3-Iodoindole (800 mg, 1 equiv), boronic acid pinacol ester (1.1 equiv) and Pd$(PPh_3)_4$ (0.05 equiv) were added to an RBF. The flask was placed under vacuum and backflushed with argon 3x. Toluene/EtOH (3:1, 40 mM to indole) was added followed by potassium carbonate (2 equiv, 2 M in water). The resulting mixture was degassed with argon for 15 min, then heated to 90 °C overnight. Following completion, the solvent was removed under reduced pressure and mixed with water and extracted 3× with EtOAc. The organic layer was washed with water and brine (2x), dried over magnesium sulfate and solvent was removed under reduced pressure. Residue was purified over silica gel with hexanes/EtOAc (6:1–2:1) to afford the product as a white solid.

***N*-Tosyl deprotection:** *N*-Tosyl-protected indole (571 mg, 1 equiv) and Cs2CO3 (3 equiv) were dissolved in THF/MeOH (3:1) (20 mM to indole) and heated to 40 °C overnight. Solvent was removed under reduced pressure followed by addition of water. Mixture was extracted with EtOAc 3x and the organic layer was washed with water and brine (2×), dried over magnesium sulfate and the solvent was removed under reduced pressure. Residue was purified over silica gel with hexanes/EtOAc (2:1) to afford the deprotected product.

4a: *N*-Benzyl-4-(6-bromo-1*H*-indol-3-yl)pyrimidin-2-amine: Produced according to the general method for 2-amino pyrimidine formation (42 mg, 8%). Tan solid. ^{1}H NMR (400 MHz, [D_4]methanol): $\delta = 8.20$ (s, 1H), 8.10 (d, $J = 5.5$ Hz, 1H), 8.01 (s, 1H), 7.56 (d, $J = 1.8$ Hz, 1H), 7.42 (d, $J = 7.6$ Hz, 2H), 7.32 (t, $J = 7.7$ Hz, 2H), 7.22 (t, $J = 7.3$ Hz, 1H), 7.14 (d, $J = 8.7$ Hz, 1H), 7.00 (d, $J = 5.5$ Hz, 1H), 4.71 (s, 2H). ^{13}C NMR (201 MHz, DMSO): $\delta = 162.7$, 162.5, 157.6, 141.3, 138.3, 138.2, 129.8, 128.6, 127.4, 126.9, 124.8, 123.5, 115.2, 114.9, 114.3, 105.7, 44.7. IR_{vmax} (cm^{-1}): 3412, 3240, 1543, 514 HRMS (ESI) for $C_{19}H_{15}BrN_4$ calculated $[M+H]^+$ 379.0553, found 379.0558. UV (λ_{max} nm) 224.

4b: 4-(6-Bromo-1*H*-indol-3-yl)-*N*-(4-chlorobenzyl)pyrimidin-2-amine: Produced according to the general method for 2-amino pyrimidine formation (35 mg, 6%). Off-white solid. ^{1}H NMR (400 MHz, [D_4]methanol): $\delta = 8.16$ (s, 1H), 8.11 (d, $J = 5.5$ Hz, 1H), 8.01 (s, 1H), 7.57 (d, $J = 1.8$ Hz, 1H), 7.40 (d, $J = 8.4$ Hz, 2H), 7.35–7.28 (m, 2H), 7.15 (d, $J = 8.7$ Hz, 1H), 7.01 (d, $J = 5.5$ Hz, 1H), 4.68 (s, 2H). ^{13}C NMR (101 MHz, DMSO): $\delta = 162.7$, 162.6, 157.6, 140.4, 138.3, 131.4, 129.8, 129.2, 128.6, 124.8, 124.4, 123.5, 115.1, 114.9, 114.3, 105.9, 44.1. $IR\nu_{max}$ (cm^{-1}): 3414, 3220, 2992, 829 HRMS (ESI) for $C_{19}H_{14}BrClN_4$ calculated $[M+H]^+$ 413.0163, found 413.0172. UV (λ_{max} nm) 220.

4c: 4-(6-Bromo-1*H*-indol-3-yl)-*N*-(4-fluorobenzyl)pyrimidin-2-amine: Produced according to the general method for 2-amino pyrimidine formation (44 mg, 8%). Tan solid. ^{1}H NMR (400 MHz, [D_6] DMSO): $\delta = 11.80$ (s, 1H), 8.24 (d, $J = 2.8$ Hz, 1H), 8.16 (d, $J = 5.3$ Hz, 2H), 7.69–7.57 (m, 2H), 7.41 (dd, $J = 8.3$, 5.5 Hz, 2H), 7.27–7.06 (m, 2H), 7.03 (d, $J = 5.3$ Hz, 1H), 4.56 (s, 2H). ^{13}C NMR (201 MHz, [D_6] DMSO): $\delta = 162.7$, 162.5, 161.5 (d, $J = 241.3$ Hz), 157.5, 138.3, 137.4 (d, $J = 3.5$ Hz), 129.8, 129.2, 124.8, 124.2, 123.5, 115.3 (d, $J = 21.2$ Hz), 115.2, 114.9, 114.3, 105.8, 43.9. IR_{vmax} (cm^{-1}): 3415, 3221, 2934, 1214 HRMS (ESI) for $C_{19}H_{14}BrFN_4$ calculated $[M+H]^+$ 397.0459, found 397.0470. UV (λ_{max} nm) 202.

4d: 4-(5-Bromo-1*H*-indol-3-yl)-*N*-(4-methylbenzyl)pyrimidin-2-amine: Produced according to the general method for 2-amino pyrimidine formation (47 mg, 9%). Tan solid. ^{1}H NMR (400 MHz, [D_4] methanol): $\delta = 8.67$ (d, $J = 1.9$ Hz, 1H), 8.08 (d, $J = 5.5$ Hz, 1H), 8.04 (s, 1H), 7.37–7.30 (m, 3H), 7.27 (dd, $J = 8.7$, 1.9 Hz, 1H), 7.12 (d, $J = 7.7$ Hz, 2H), 6.98 (d, $J = 5.5$ Hz, 1H), 4.68 (s, 2H), 2.29 (s, 3H). ^{13}C NMR (201 MHz, DMSO): $\delta = 162.8$, 162.5, 157.7, 138.2, 136.9, 135.8, 130.3, 129.3, 129.3, 129.2, 127.5, 127.3, 125.06, 114.3, 113.7, 105.5, 44.3, 21.1. IR_{vmax} (cm^{-1}): 3394, 3165, 2924, 1525 HRMS (ESI) for $C_{20}H_{17}BrN_4$ calculated $[M+H]^+$ 393.0709, found 393.0730. UV (λ_{max} nm) 220.

4e: 4-(5-Bromo-1*H*-indol-3-yl)-*N*-(4-methoxybenzyl)pyrimidin-2-amine: Produced according to the general method for 2-amino pyrimidine formation (30 mg, 5%). Tan solid. ^{1}H NMR (400 MHz, [D_4] methanol): $\delta = 8.69$ (d, $J = 2.0$ Hz, 1H), 8.08 (dd, $J = 5.5$, 1.5 Hz, 1H), 8.04 (d, $J = 2.4$ Hz, 1H), 7.43–7.22 (m, 4H), 6.98 (dd, $J = 5.5$, 2.3 Hz, 1H), 6.90–6.82 (m, 2H), 4.65 (s, 2H), 3.75 (d, $J = 1.4$ Hz, 3H). ^{13}C NMR

(201 MHz, DMSO): δ = 162.8, 162.7, 162.5, 158.4, 157.7, 136.2, 133.2, 130.3, 130.1, 128.6, 127.5, 125.0, 114.3, 114.1, 113.7, 105.4, 55.4, 43.9. IR_{vmax} (cm^{-1}): 3415, 3119, 2927, 1217 HRMS (ESI) for $C_{20}H_{17}BrN_4O$ calculated $[M+H]^+$ 409.0658, found 409.0650. UV (λ_{max} nm) 222.

4 f: *N*-(4-Aminobenzyl)-4-(5-bromo-1*H*-indol-3-yl)pyrimidin-2-amine: Produced according to the modified method for 2-amino pyrimidine formation. Purified over silica using 3% methanol saturated with ammonia in CH_2Cl_2 (33 mg, 6%). Tan solid. ^{1}H NMR (400 MHz, [D_4]methanol): δ = 8.71 (d, J = 1.9 Hz, 1H), 8.07 (d, J = 5.5 Hz, 1H), 8.04 (s, 1H), 7.34 (d, J = 8.6 Hz, 1H), 7.27 (dd, J = 8.7, 2.0 Hz, 1H), 7.25–7.15 (m, 2H), 6.97 (d, J = 5.5 Hz, 1H), 6.81–6.64 (m, 2H), 4.59 (s, 2H). ^{13}C NMR (101 MHz, DMSO): δ = 162.8, 162.5, 157.6, 147.7, 136.2, 136.0, 130.2, 130.1, 128.5, 128.2, 127.5, 125.1, 114.3, 114.2, 113.9, 113.7, 105.3, 44.3. IR_{vmax} (cm^{-1}): 3394, 3386, 3019, 2920 HRMS (ESI) for $C_{19}H_{16}BrN_5$ calculated $[M+H]^+$ 394.0662, found 394.0669. UV (λ_{max} nm) 222.

4 g: 4-(5-Bromo-1*H*-indol-3-yl)-*N*-(4-(trifluoromethyl)benzyl)pyrimidin-2-amine: Produced according to the general method for 2-amino pyrimidine formation (45 mg, 7%). Tan solid. ^{1}H NMR (400 MHz, [D_4]methanol): δ = 8.56 (s, 1H), 8.10 (d, J = 5.5 Hz, 1H), 8.04 (s, 1H), 7.61 (d, J = 2.2 Hz, 4H), 7.32 (d, J = 8.6 Hz, 1H), 7.25 (dd, J = 8.6, 2.0 Hz, 1H), 7.01 (d, J = 5.5 Hz, 1H), 4.81 (s, 2H). ^{13}C NMR (201 MHz, [D_6]DMSO): δ = 162.7, 162.4, 157.9, 146.3, 136.2, 130.4, 130.3, 127.8, 127.7, 127.5 (d, J = 19.2 Hz), 127.4, 125.6, 125.1, 124.9 (q, J = 272.0 Hz), 114.3, 113.7, 105.9, 44.3. IR_{vmax} (cm^{-1}): 3251, 3088, 2908, 1326 HRMS (ESI) for $C_{20}H_{14}BrF_3N_4$ calculated $[M+H]^+$ 447.0427, found 447.0420. UV (λ_{max} nm) 220.

4 h: 4-(5-Bromo-1*H*-indol-3-yl)-*N*-(4-chlorobenzyl)pyrimidin-2-amine: Produced according to the general method for 2-amino pyrimidine formation (34 mg, 6%). Tan solid. ^{1}H NMR (400 MHz, [D_4]methanol): δ = 8.61 (s, 1H), 8.10 (d, J = 5.5 Hz, 1H), 8.05 (s, 1H), 7.43 (d, J = 8.2 Hz, 2H), 7.37–7.23 (m, 4H), 7.00 (d, J = 5.5 Hz, 1H), 4.71 (s, 2H). ^{13}C NMR (201 MHz, DMSO): δ = 162.7, 162.5, 157.9, 140.4, 136.2, 131.4, 130.4, 129.3, 129.0, 128.6, 127.4, 125.1, 124.8, 114.3, 113.7, 105.7, 43.9. IR_{vmax} (cm^{-1}): 3411, 3015, 2925, 791 HRMS (ESI) for $C_{19}H_{14}BrClN_4$ calculated $[M+H]^+$ 413.0163, found 413.0169. UV (λ_{max} nm) 218.

4 i: 4-(5-Bromo-1*H*-indol-3-yl)-*N*-(4-bromobenzyl)pyrimidin-2-amine: Produced according to the general method for 2-amino pyrimidine formation (37 mg, 6%). Tan solid. ^{1}H NMR (400 MHz, [D_4]methanol): δ = 8.60 (s, 1H), 8.09 (d, J = 5.4 Hz, 1H), 8.03 (s, 1H), 7.48–7.23 (m, 6H), 6.99 (d, J = 5.5 Hz, 1H), 4.68 (s, 2H). ^{13}C NMR (101 MHz, DMSO): δ = 162.7, 157.5, 140.8, 136.2, 131.8, 131.5, 130.4, 129.5, 127.4, 125.1, 124.8, 119.8, 114.3, 113.8, 113.7, 105.7, 44.0. IR_{vmax} (cm^{-1}): 3420, 3103, 2919, 657 HRMS (ESI) for $C_{19}H_{14}Br_2N_4$ calculated $[M+H]^+$ 456.9658, found 456.9659. UV (λ_{max} nm) 226.

4 j: 4-(5-Bromo-1*H*-indol-3-yl)-*N*-(3-(trifluoromethyl)benzyl)pyrimidin-2-amine: Produced according to the general method for 2-amino pyrimidine formation (39 mg, 7%). Tan solid. ^{1}H NMR (400 MHz, [D_4]methanol): δ = 8.59 (s, 1H), 8.11 (d, J = 5.4 Hz, 1H), 8.03 (s, 1H), 7.76–7.68 (m, 2H), 7.57–7.44 (m, 2H), 7.32 (d, J = 8.6 Hz, 1H), 7.25 (dd, J = 8.6, 2.0 Hz, 1H), 7.00 (d, J = 5.5 Hz, 1H), 4.80 (s, 2H). ^{13}C NMR (101 MHz, [D_6]DMSO): δ = 162.7, 157.9, 142.9, 136.2, 131.4, 130.4, 129.7, 129.5, 129.4, 127.4, 126.8, 125.1, 124.8 (q, J = 272.2 Hz), 123.7 (d, J = 4.1 Hz), 122.8, 114.3, 113.7, 105.9, 44.2. IR_{vmax} (cm^{-1}): 3134, 3075, 2917, 1328 HRMS (ESI) for $C_{20}H_{14}BrF_3N_4$ calculated $[M+H]^+$ 447.0427, found 447.0421. UV (λ_{max} nm) 220.

4 k: 4-(5-Bromo-1*H*-indol-3-yl)-*N*-(3-methoxybenzyl)pyrimidin-2-amine: Produced according to the general method for 2-amino pyrimidine formation (43 mg, 8%). Tan solid. ^{1}H NMR (400 MHz, [D_4]methanol): δ = 8.68 (d, J = 2.0 Hz, 1H), 8.10 (d, J = 5.5 Hz, 1H), 8.05 (s, 1H), 7.39–7.16 (m, 3H), 7.10–6.96 (m, 3H), 6.83–6.71 (m, 1H), 4.71 (s, 2H), 3.73 (s, 3H). ^{13}C NMR (201 MHz, [D_6]DMSO): δ = 168.0, 159.9, 154.4, 144.6, 140.0, 136.8, 136.7, 130.2, 127.2, 126.4, 124.8, 119.5, 115.5, 115.2, 113.0, 112.9, 112.8, 105.4, 55.5, 44.6. HRMS (ESI) for $C_{20}H_{17}BrN_4O$ calculated $[M+H]^+$ 409.0658, found 409.0659. UV (λ_{max} nm) 220. R_f: 0.15 (hexanes/ethyl acetate 1:2).

4 l: 4-(5-Bromo-1*H*-indol-3-yl)-*N*-(3-methylbenzyl)pyrimidin-2-amine: Produced according to the general method for 2-amino pyrimidine formation (49 mg, 9%). Tan solid. ^{1}H NMR (400 MHz, [D_4] methanol): δ = 8.68 (d, J = 2.0 Hz, 1H), 8.09 (d, J = 5.5 Hz, 1H), 8.05 (s, 1H), 7.37–7.15 (m, 5H), 7.03 (d, J = 7.4 Hz, 1H), 6.99 (d, J = 5.5 Hz, 1H), 4.70 (s, 2H), 2.31 (s, 3H). ^{13}C NMR (201 MHz, DMSO): δ = 162.8, 162.5, 157.7, 141.2, 137.6, 136.2, 130.3, 130.2, 128.6, 128.0, 127.6, 127.5, 127.4, 125.0, 124.5, 114.3, 113.7, 105.5, 44.5, 21.6. HRMS (ESI) for $C_{20}H_{17}BrN_4$ calculated $[M+H]^+$ 393.0709, found 393.0713. UV (λ_{max} nm) 224. R_f: 0.2 (hexanes/ethyl acetate 1:2).

4 m: 4-(5-Bromo-1*H*-indol-3-yl)-*N*-(naphthalen-1-ylmethyl)pyrimidin-2-amine: Produced according to the general method for 2-amino pyrimidine formation (33 mg, 6%). Tan solid. ^{1}H NMR (400 MHz, [D_4]methanol): δ = 8.57 (s, 1H), 8.22 (dt, J = 410.8, 8.9, 8.2 Hz, 1H), 8.14 (d, J = 5.5 Hz, 1H), 8.07 (s, 1H), 7.97–7.88 (m, 1H), 7.79 (d, J = 8.3 Hz, 1H), 7.62–7.47 (m, 3H), 7.43 (dd, J = 8.2, 7.1 Hz, 1H), 7.31 (d, J = 8.6 Hz, 1H), 7.21 (dd, J = 356.6, 12.6 Hz, 1H), 7.03 (d, J = 5.5 Hz, 1H), 5.22 (s, 2H). ^{13}C NMR (101 MHz, DMSO): δ = 162.4, 162.4, 162.2, 157.0, 135.7, 135.5, 133.4, 131.0, 129.9, 129.7, 128.5, 127.0, 127.0, 126.1, 125.7, 125.4, 124.6, 123.4, 113.8, 113.3, 113.2, 105.3, 42.2. IR_{vmax} (cm^{-1}): 3087, 3036, 2907, 2879 HRMS (ESI) for $C_{23}H_{17}BrN_4$ calculated $[M+H]^+$ 429.0709, found 429.0710. UV (λ_{max} nm) 224.

4 n: 4-(5-Bromo-1*H*-indol-3-yl)-*N*-(3,5-dimethylbenzyl)pyrimidin-2-amine: Produced according to the general method for 2-amino pyrimidine formation (45 mg, 8%). White solid. ^{1}H NMR (400 MHz, [D_4]methanol): δ = 8.70 (d, J = 2.0 Hz, 1H), 8.09 (d, J = 5.5 Hz, 1H), 8.05 (s, 1H), 7.34 (d, J = 8.6 Hz, 1H), 7.27 (dd, J = 8.7, 2.0 Hz, 1H), 7.06 (s, 2H), 6.99 (d, J = 5.5 Hz, 1H), 6.85 (s, 1H), 4.66 (s, 2H), 2.27 (s, 6H). ^{13}C NMR (101 MHz, DMSO): δ = 162.8, 162.5, 157.5, 141.2, 137.5, 136.2, 130.3, 130.2, 128.4, 127.5, 125.1, 124.7, 114.3, 113.8, 113.7, 105.4, 44.5, 21.5. HRMS (ESI) for $C_{21}H_{16}BrN_4$ calculated $[M+H]^+$ 407.0866, found 407.0865. UV (λ_{max} nm) 200. R_f: 0.2 (hexanes/ethyl acetate 1:1).

6 a: *N*-Benzyl-5-(5-bromo-1*H*-indol-3-yl)pyrimidin-2-amine: Produced according to the general Tosyl deprotection (380 mg, 94%). White solid. ^{1}H NMR (400 MHz, [D_4]methanol): δ = 8.53 (s, 2H), 7.80 (d, J = 1.8 Hz, 1H), 7.48 (s, 1H), 7.43–7.19 (m, 7H), 4.65 (s, 2H). ^{13}C NMR (101 MHz, DMSO): δ = 160.8, 155.8, 140.6, 135.3, 128.2, 127.0, 126.7, 126.5, 124.1, 124.0, 121.0, 117.8, 113.9, 112.2, 109.9, 44.0. IR_{vmax} (cm^{-1}): 3221, 3206, 2935, 1457 HRMS (ESI) for $C_{19}H_{15}BrN_4$ calculated $[M+H]^+$ 379.0553, found 379.0556. UV (λ_{max} nm) 206.

6 b: 4-(((5-(5-Bromo-1*H*-indol-3-yl)pyrimidin-2 yl)amino)methyl) benzonitrile: Produced according to the general Tosyl deprotection (361 mg, 95%). White solid. ^{1}H NMR (400 MHz, [D_4]methanol): δ = 8.54 (s, 2H), 7.79 (d, J = 1.8 Hz, 1H), 7.74–7.64 (m, 2H), 7.56 (d, J = 8.1 Hz, 2H), 7.48 (s, 1H), 7.36 (d, J = 8.7 Hz, 1H), 7.26 (dd, J = 8.7, 1.8 Hz, 1H), 4.72 (s, 2H). ^{13}C NMR (201 MHz, DMSO): δ = 161.1, 156.3, 147.2, 135.8, 132.7, 128.2, 127.2, 124.6, 124.5, 121.4, 119.5, 118.6, 114.3, 112.7, 110.3, 109.7, 44.4. IR_{vmax} (cm^{-1}): 3278, 3087, 2228, 1457 HRMS (ESI) for $C_{20}H_{14}BrN_5$ calculated $[M+H]^+$ 404.0505, found 404.0511. UV (λ_{max} nm) 228.

6 c: Methyl 4-(((5-(5-bromo-1*H*-indol-3-yl)pyrimidin-2-yl)amino) methyl)benzoate: Produced according to the general Tosyl deprotection (303 mg, 96%). White solid. ^{1}H NMR (400 MHz, [D_4] methanol): δ = 8.54 (s, 2H), 8.04–7.95 (m, 2H), 7.80 (d, J = 1.8 Hz, 1H), 7.58–7.46 (m, 3H), 7.36 (d, J = 8.6 Hz, 1H), 7.26 (dd, J = 8.6, 1.9 Hz, 1H), 4.72 (s, 2H), 3.89 (s, 3H). ^{13}C NMR (201 MHz, DMSO): δ =

166.6, 161.2, 156.3, 146.9, 135.8, 129.7, 128.4, 127.6, 127.2, 124.6, 124.5, 121.4, 118.5, 114.3, 112.6, 110.3, 52.5, 44.4. IR_{vmax} (cm^{-1}): 3152, 2986, 1705, 1281 HRMS (ESI) for $C_{21}H_{17}BrN_4O_2$ calculated $[M+H]^+$ 437.0608, found 437.0608. UV (λ_{max} nm) 232.

6 d: 5-(5-Bromo-1*H*-indol-3-yl)-*N*-(4-chlorobenzyl)pyrimidin-2-amine: Produced according to the general Tosyl deprotection (345 mg, 92%). White solid. ^1H NMR (400 MHz, [D_4]methanol): $\delta=$ 8.53 (s, 2H), 7.80 (d, $J=1.8$ Hz, 1H), 7.48 (s, 1H), 7.42–7.23 (m, 6H), 4.63 (s, 2H). ^{13}C NMR (101 MHz, DMSO): $\delta=160.7$, 155.8, 139.7, 135.3, 131.0, 128.9, 128.1, 126.7, 124.1, 124.1, 121.0, 118.0, 113.9, 112.2, 109.9, 43.5. IR_{vmax} (cm^{-1}): 3421, 3104, 3005, 624 HRMS (ESI) for $C_{19}H_{14}BrClN_4$ calculated $[M+H]^+$ 413.0163, found 413.0153. UV (λ_{max} nm) 220.

6 e: 5-(5-Bromo-1*H*-indol-3-yl)-*N*-(4-fluorobenzyl)pyrimidin-2-amine: Produced according to the general Tosyl deprotection (320 mg, 86%). White solid. ^1H NMR (400 MHz, [D_4]methanol): $\delta=$ 8.54 (s, 2H), 7.81 (d, $J=1.9$ Hz, 1H), 7.49 (s, 1H), 7.46–7.33 (m, 3H), 7.28 (dd, $J=8.6$, 1.9 Hz, 1H), 7.11–6.99 (m, 2H), 4.63 (s, 2H). ^{13}C NMR (201 MHz, [D_6]DMSO): $\delta=161.80$ (d, $J=242.3$ Hz), 156.0, 135.8, 135.3, 129.8, 129.8 (d, $J=8.0$ Hz), 126.8, 125.8, 124.8, 121.5, 118.6, 115.6 (d, $J=21.2$ Hz), 114.5, 113.0, 108.2, 44.0. IR_{vmax} (cm^{-1}): 3469, 3165, 2919, 1213 HRMS (ESI) for $C_{19}H_{14}BrFN_4$ calculated $[M+H]^+$ 397.0459, found 397.0472. UV (λ_{max} nm) 228.

General biological procedures: *M. smegmatis* strain (ATCC 700084, mc2155) was obtained from ATCC (Manassas, VA). *A. baumannii* strain 4106 was obtained from Walter Reed Army Institute of Research, *K. pneumoniae* strain B9 was obtained from Prof. Robert Ernst at The University of Maryland, Baltimore. Stock cultures were stored as glycerol stocks (25% *v/v* glycerol and 7H9 (BD cat# 271310), ADC (BD cat# 211887), Tween 80 (*M. smegmatis*) or 25% *v/v* glycerol and LB Gram-negative strains) and maintained at −80 °C. *M. smegmatis* was cultured in 7H9 and plated on 7H10 agar (OADC, glycerol) Gram-negative strains were plated on LB (Lennox) agar. M9 minimal salts media was purchased from BD Diagnostics (cat# 248510). Cation adjusted mueller hinton broth (CAMHB) was purchased from BD Diagnostics (cat# 212322). Colistin sulfate was purchased from Sigma (cat# C4461). All assays were run in duplicate and repeated at least two separate times. All compounds were dissolved as their HCl salts in molecular biology grade DMSO as 10 or 100 mM stock solutions and stored at −20 °C.

Broth microdilution method for MIC determination (*A. baumannii, K. pneumoniae*): Overnight cultures of bacterial strain were subcultured to 5×10^5 CFU/mL in cation-adjusted Mueller–Hinton medium. The resulting bacterial suspension was aliquoted (1.0 mL) into culture tubes. Samples were prepared from these culture tubes containing either 200 μmol of specified antibiotic or no test compound as a control. Samples were then aliquoted (200 μL) into the first row of wells of a 96-well microtiter plate in which subsequent wells were prefilled with 100 μL of Mueller–Hinton medium based 5×10^5 CFU/mL bacterial subculture. Using the multichannel pipettor set at 100 μL, row 1 wells were mixed 8–10 times. Then, 100 μL were withdrawn and transferred to row two. Row 2 wells were mixed 8–10 times followed by a 100 μL transfer from row 2 to row 3. This procedure was used to serial dilute the rest of the rows of the microtiter plate. The microtiter plate sample was then covered with a microtiter plate lid and then placed in a covered plastic container. The chamber was incubated under stationary conditions at 37 °C. After 16 h, the lid was removed, and MIC values were recorded.

Broth microdilution method for MIC determination of *M. smegmatis* Cultures: (ATCC 700084, mc2155; 48 h) were standardized to 5×10^5 CFU/mL in 7H9 broth supplemented with ADC enrichment. Aliquots (1 mL) were placed in culture tubes, and compound was added from 100 mM stock samples in DMSO, such that the compound concentration equaled the highest concentration tested (200 μM). Samples were then aliquoted (200 μL) into the first row of wells of a 96-well plate, with all remaining wells being filled with 100 μL of initial bacterial subculture. Row 1 wells were mixed five times before 100 μL was transferred to the following row (row 2). Row 2 was then mixed five times, and 100 μL was transferred to row 3. This process provided a serial dilution of the compound and was continued until the final row had been mixed. Plates were covered with Glad Press n′ Seal and were incubated under stationary conditions at 37 °C for 48 h. After 48 h, the wells were stained with 10 μL of alamarBlue (Thermo-Fisher) and were incubated under stationary conditions at 37 °C for 8 hours. After 8 h, the wells with viable bacteria were visualized as pink and the wells with no viable bacteria were visualized as blue. MIC values were recorded as the lowest concentration at which no viable bacteria were observed.

Broth microdilution method for antibiotic re-sensitization: Overnight cultures of bacteria in cation adjusted Mueller-Hinton Broth (CAMHB) were subcultured to 5×10^5 CFU/mL in CAMHB. Aliquots (5 mL) were placed in culture tubes and dosed with compound from stock solutions to give concentrations of 30% of the MIC of the compound against the particular bacterial strain. One milliliter of the resulting solution was placed in a separate culture and dosed with antibiotic at the highest concentration to be tested. Bacteria treated with antibiotic alone were used as the control. Row 1 of a 96-well plate was filled with 200 μL of the antibiotic/adjuvant, and rows 2–8 were filled with 100 μL each of the remaining 4 mL of bacterial subculture. Row 1 was then mixed five times, and 100 μL was transferred to row 2, which was then mixed five times before being transferred to row 3. This process was repeated until all rows had been mixed, except for row 8, which would have only compound, to serve as a control. The 96-well plate was then covered in Glad Press n′ Seal and incubated under stationary conditions at 37 °C for 16 h. MIC values were determined as the lowest concentration at which no bacterial growth was observed; fold reductions were determined by comparison to control lane.

Biofilm inhibition assay: *M. smegmatis* was grown in 7H9 (ADC, 0.5% Tween 80) for 48 h and this culture was used to inoculate Difco M9 minimal salts medium ($OD_{600}=0.01$) supplemented with glucose (20% Sigma-Aldrich, 2 mL per 100 mL), $MgSO_4$ (1 M, 200 μL per 100 mL), and $CaCl_2$ (1 M, 10 μL per 100 mL). 100 μL per well of the subculture was aliquoted into the center two columns of a 96-well PVC microtiter plate. Columns 1 and 12 served as negative control wells. Then compound from DMSO stock solutions was added to aliquots of the subculture to give the desired concentration to be tested and aliquoted (100 μL per well) into the remaining wells of the 96-well PVC microtiter plate. Sample plates were then wrapped in GLAD Press n'Seal and were incubated under stationary conditions for 48 h at 37 °C. After incubation, the medium was discarded, and the plates were washed thoroughly with water. The wells were stained with 110 μL of a 0.1% solution of crystal violet and then left at ambient temperature for 30 min. Crystal violet solution was discarded and plates washed thoroughly with water. 200 μL of 95% ethanol was added to each well, and the plates left covered at ambient temperature for 10 min. 125 μL of the ethanol solution was transferred to a polystyrene microtiter plate. Biofilm inhibition was quantified by measuring the OD_{540} of each well. The values obtained from the two negative control lanes were subtracted from the OD_{540} of the other columns.

Acknowledgements

The authors would like to thank the National Institutes of Health (AI106733 and AI136904) for funding.

Conflict of Interest

Dr. Christian Melander is the co-founder of Agile Sciences Inc., which focuses on harnessing small molecules to combat biofilms and antibiotic resistance.

Keywords: Adjuvants · antibiotic resistance · biofilms · colistin · Gram-negative bacteria

[1] M. Woolhouse, C. Waugh, M. R. Perry, H. Nair, *J. Glob. Health* **2016**, *6*, 010306.
[2] Center for Disease Control and Prevention, *Antibiotic Resistance Threats In The United States*, **2019**.
[3] A. O. Javan, S. Shokouhi, Z. Sahraei, *Eur. J. Clin. Pharmacol.* **2015**, *71*, 801–810.
[4] R. J. Worthington, J. J. Richards, C. Melander, *Org. Biomol. Chem.* **2012**, *10*, 7457–74.
[5] D. F. Ackart, L. Hascall-Dove, S. M. Caceres, N. M. Kirk, B. K. Podell, C. Melander, I. M. Orme, J. G. Leid, J. A. Nick, R. J. Basaraba, *Pathog Dis* **2014**, *70*, 359–369.
[6] World Health Organization, *Global Tuberculosis Report*, **2019**.
[7] K. E. Cox, C. Melander, *MedChemComm* **2019**, *10*, 1177–1179.
[8] A. B. Jeon, D. F. Ackart, W. Li, M. Jackson, R. J. Melander, C. Melander, C. R. B. Abramovitch, A. J. Chicco, R. J. Basaraba, A. Obregon-Henao, *Sci. Rep.* **2019**, *9*, 1513.
[9] A. B. Jeon, A. Obregon-Henao, D. F. Ackart, B. K. Podell, J. M. Belardinelli, M. Jackson, T. V. Nguyen, M. S. Blackledge, R. J. Melander, C. Melander, B. K. Johnson, R. B. Abramovitch, R. J. Basaraba, *PLoS One* **2017**, *12*, e0180925.
[10] S. M. Brackett, K. E. Cox, S. L. Barlock, W. M. Huggins, D. F. Ackart, R. J. Bassaraba, R. J. Melandera, C. Melander, *RSC Med. Chem.* **2019**, *2020*, 92–97.
[11] W. M. Huggins, W. T. Barker, J. T. Baker, N. A. Hahn, R. J. Melander, C. Melander, *ACS Med. Chem. Lett.* **2018**, *9*, 702–707.
[12] T. Ito, M. Murai, H. Morisaka, H. Miyoshi, *Biochemistry* **2015**, *54*, 3677–86.
[13] Q. Zhou, A. F. Phoa, R. H. Abbassi, M. Hoque, T. A. Reekie, J. S. Font, R. M. Ryan, B. W. Stringer, B. W. Day, T. G. Johns, L. Munoz, M. Kassiou, *J. Med. Chem.* **2017**, *60*, 2052–2070.
[14] M. Murata, T. Oyama, S. Watanabe, Y. Masuda, *J. Org. Chem.* **2000**, *65*, 164–8.
[15] S. B. Joginder, G. P. Chen, K. Prasad, O. Repic, T. J. Blacklock, *Tetrahedron Lett.* **2006**, *47*, 6425–6427.

Manuscript received: June 18, 2020
Accepted manuscript online: July 14, 2020
Version of record online: ■■, ■■■

FULL PAPERS

Providing backup: Structure-activity relationship studies were performed on an analogue of the natural product meridianin D. Members of the library exhibited increased inhibitory activity against *M. smegmatis* biofilms as well as the ability to potentiate colistin against two clinically relevant polymyxin-resistant bacterial strains.